

PAPER • OPEN ACCESS

Structural and micromechanical properties of 316L stainless steel produced by selective laser melting

To cite this article: A V Makarov *et al* 2020 *IOP Conf. Ser.: Mater. Sci. Eng.* **1008** 012005

View the [article online](#) for updates and enhancements.



The Electrochemical Society
Advancing solid state & electrochemical science & technology
2021 Virtual Education

Fundamentals of Electrochemistry:
Basic Theory and Kinetic Methods
Instructed by: **Dr. James Noël**
Sun, Sept 19 & Mon, Sept 20 at 12h–15h ET

Register early and save!



Structural and micromechanical properties of 316L stainless steel produced by selective laser melting

A V Makarov¹, V P Kuznetsov^{1,2}, V A Sirosh¹, E G Volkova¹, P A Skorynina³ and A G Merkushev²

¹M .N. Miheev Institute of Metal Physics, Ural Branch of the Russian Academy of Sciences, 18 S. Kovalevskoy St., Ekaterinburg, 620108, Russia

²Ural Federal University, 19 Mira St., Ekaterinburg, 620002 Russia

³Institute of Engineering Science, Ural Branch of the Russian Academy of Sciences, 34 Komsomolskaya St., Ekaterinburg, 620049, Russia

E-mail: sirosh@imp.uran.ru

Abstract. The structure and micromechanical properties of a 316L stainless steel produced by the selective laser melting (SLM) technique have been studied in its initial state and the following heat treatment: quenching from 1050 °C and 4-hour annealing at 480 °C. The heat treatment does not result in changing the steel phase composition, however, it reduces the microhardness by 5%, *HM* hardness (Martens hardness) by 12% and indentation hardness by 16% at H_{IT} maximum load. The heat treatment also increases the E^* contact elasticity modulus by 14% due to the lower porosity of the material. As soon as heat treatment provides no strengthening of the steel synthesized by SLM, deformation processing, chemicothermal treatment and application of thin coatings may become quite promising strengthening methods.

1. Introduction

Additive manufacturing has been gaining a solid ground in modern engineering. This rapidly progressing technology proves to be the most promising for the fabrication of complex parts in the aeronautic, automotive, medical industries, etc. Selective laser melting is one of its applications, which is the layer-after-layer formation of a piece by laser beam scanning of powder layers laid on a substrate. As layers are added, different parts of the piece are subjected to various thermal effects. This leads to residual stresses caused by temperature gradients between the layers. This effect is likely to initiate cracking and delamination of the material [1]. The combination of incomplete fusion [2] and residual stresses brings about high porosity inside the part. Hence, the application of post-processing (deformation processing, heat and chemicothermal treatments, deposition of coating) designed to improve the quality of the material is topical for parts synthesized by the SLM technique.

The purpose of the study was looking into the structural phase states and micromechanical characteristics of stainless chrome-nickel steel samples produced by SLM, including those that were subjected to post-heat treatment.

2. Materials and methods

Stainless austenitic steel samples produced by SLM were studied, their chemical composition being



Content from this work may be used under the terms of the [Creative Commons Attribution 3.0 licence](https://creativecommons.org/licenses/by/3.0/). Any further distribution of this work must maintain attribution to the author(s) and the title of the work, journal citation and DOI.

(mass) Cr 15.93%; Ni 10.00%; Mo 2.20%; Mn 1.27%; Si 0.55%; C 0.03%; S 0.02%; P 0.08%, Fe – the rest. An EOS M 280 unit was used to build the samples in gaseous nitrogen employing a 400W laser; the diameter of the laser spot on the surface was 50 μ m, the thickness of the applied powder layer - 20 μ m, the rate of the laser beam movement on the powder surface reaching 1000 mm/sec. The structure and micromechanical properties of the steel were investigated in its initial state after forming the samples by the SLM technique and subsequent heat treatment. The aim of heat treatment (HT) was to degass and reduce the amount of vacancies, and to relax residual stresses in the synthesized sample. It was heat treated at 1050 °C for 30 minutes, followed by oil quenching with subsequent 4-hrs ageing at 480 °C and air cooling.

A JEOL JEM-200CX transmission electron microscope was used to study the steel structure. To determine the microhardness, a Shumadzu HMV-G21DT device as well as the residual imprint method were utilized with a load on the Vickers indenter of 0.245 N. An ISO 14577 Fischerscope HM2000 XYm measurement system was applied to determine the microindentation characteristics. The maximum microindentation load on the Vickers indenter was 0.245 N. The micromechanics of the coatings were found with the help of loading and unloading curves gained by the Oliver-Pharr method [3].

3. Experimental results and discussion

The transmission electron microscope survey showed that the initial structure of the 316L steel samples in the planes cut parallel (\parallel) and perpendicular (\perp) to the Z axis (figure 1), i.e. parallel and perpendicular to the sample building direction during the SLM process, prior to the heat treatment was identical. The structure consists of elongated subgrains with separate dislocations or dislocation cells inside them (figure 2). All the grains were γ -Fe (austenite).

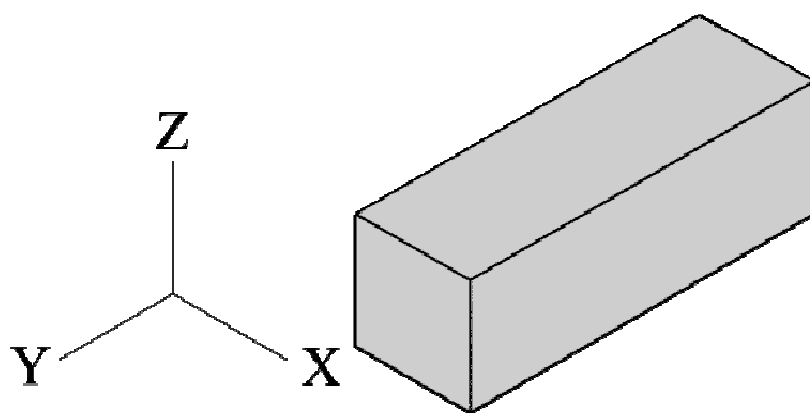


Figure 1. Schematic illustration of the sample synthesis: X,Y - scanning direction, Z - building direction.

The structure of the heat-treated steel in the vertical plane parallel to the Z axis, i.e. in the direction of the sample building (\parallel), comprises elongated austenitic subgrains with prolonged, straight, band-shaped boundaries (figure 3). The density of dislocations inside the grains is low.

The results of the structural survey fully agree with the published data on the cellular structure in 316L stainless steel formed by SLM [4-6]. The 30 minutes annealing at 1050 °C prior to quenching is expected to make gaseous impurities, which are likely to have evolved during the SLM process, to emit from the γ -solid solution [6]. Uneven distribution of powder in SLM could have led to the formation of the ferrite phase [7], but no α -phase was detected.

The microhardness tests applying the recovered indentation technique revealed that heat treatment results in a slight softening of the steel; the microhardness decreased by 5% from 252 \pm 7 HV 0.025 to 240 \pm 5 HV 0.025.

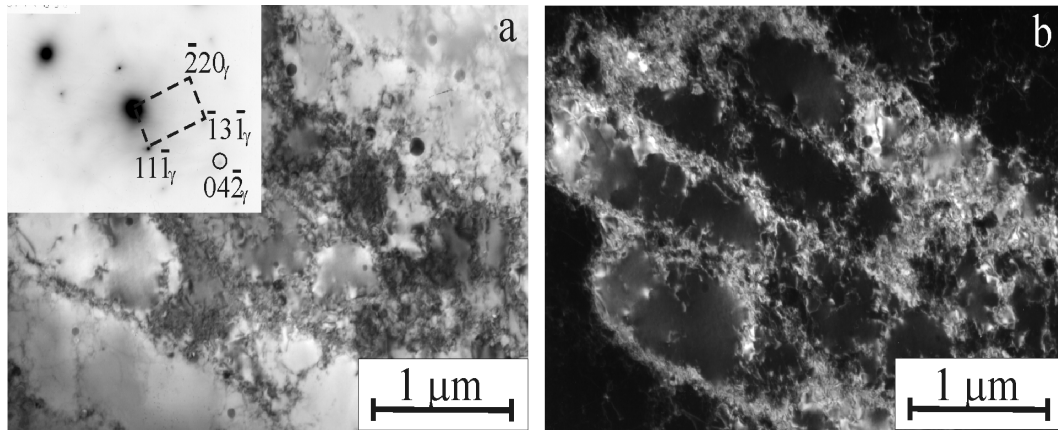


Figure 2. TEM images of the initial 316L (II) SLM samples structure: bright field and electronic diffraction patterns (a), dark field (b).

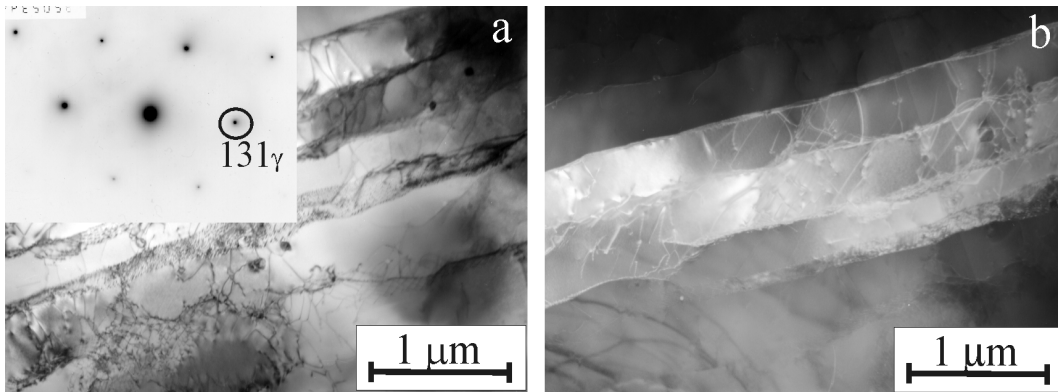


Figure 3. TEM images of the 316L (II) SLM samples structure after heat treatment: bright field and electronic diffraction patterns (a), dark field (b).

Figure 4 shows the diagrams that describe the loading, namely, the ascending curve, and unloading, represented by the distending curve, at the maximum load $F = 0.245$ N as determined by the instrumental microindentation method. It is evident that the heat treatment results in shifting the curves towards higher values of the thrust of the indenter h to the right; consequently the values of the maximal (h_{max}) and residual (h_p) indentation depths rise by 7% and 10% respectively, see table 1. The lower strength properties also prove that the material becomes softer (table 1); namely, the Martens hardness HM revealing both plastic and elastic deformations decreases by 12%, from 2.72 ± 0.07 GPa to 2.39 ± 0.05 GPa while the indentation hardness at the maximum load H_{IT} drops by 16% from 3.18 ± 0.09 GPa to 2.67 ± 0.06 GPa. This slight softening of the steel may be attributed to the above-mentioned lower density of dislocations following the heat treatment. It is significant to note that the microindentation data shows higher values of the contact elasticity modulus E^* ; it rose by 14% from 171 GPa to 195 GPa (table 1). It reflects a lower porosity (compaction) of the synthesized steel resulting from high temperature heating.

The total mechanical work of indentation W_t determined by the area under the loading curve in figure 4 including the work spent for plastic deformation and elastic recovery, also rises by 8% after heat treatment (table 1), since the less the strength of material, the higher is its deformation under the indenter and consequently the more work is done on deformation. The work of elastic deformation W_e determined by the area under the unloading curve in figure 4, on the contrary, goes down by 16%. The fraction of the elastic deformation in the total deformation decrease; it is also proved by the lower

values of the relation H_{IT}/E^* [8] and the elastic recovery $R = ((h_{max} - h_p)/h_{max}) \times 100\%$ [9] that decrease by 26 and 19%, respectively (table 2). Somehow, the plastic component of the work of indentation calculated using the formula $\delta A = (1 - (W_e/W_t)) \times 100\%$ [10] grows very insignificantly, by 3.5%, and the resistance to deformation after the transition to plastic flow, which is described by the relation H_{IT}^3/E^{*2} [11], does not change after heat treatment at all (table 2).

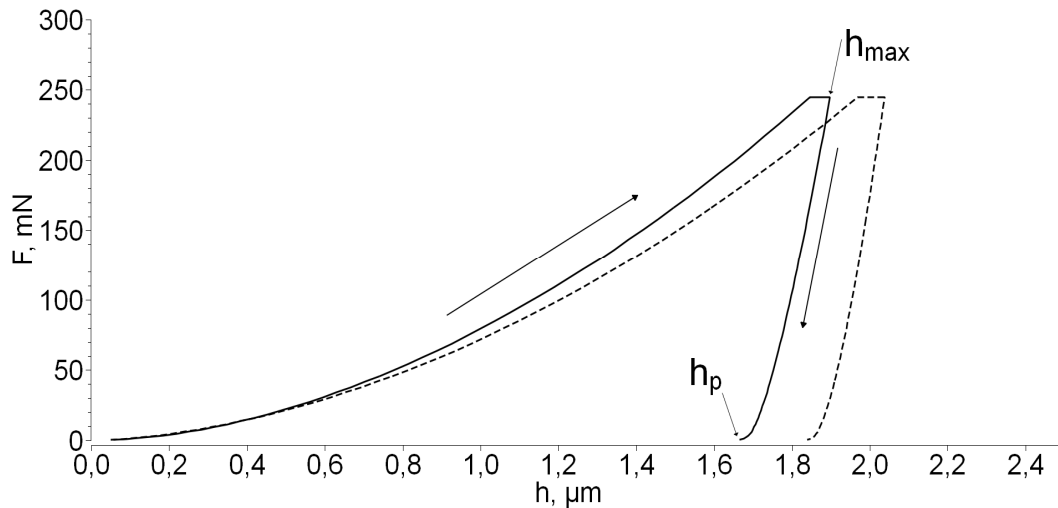


Figure 4. Experimental curves during microindentation of the 316L SLM samples surfaces after (dash-line) and without (solid line) heat treatment.

Table 1. The surfaces microindentation results of 316L SLM samples after and without heat treatment.

Treatment	h_{max} (μm)	h_p (μm)	HM (GPa)	H_{IT} (GPa)	E^* (GPa)	W_t (nJ)	W_e (nJ)
Without HT	1.90 ± 0.03	1.67 ± 0.02	2.72 ± 0.07	3.18 ± 0.09	171 ± 4	159.1 ± 2.8	22.0 ± 0.5
After HT	2.04 ± 0.02	1.84 ± 0.02	2.39 ± 0.05	2.67 ± 0.06	195 ± 5	171.8 ± 1.9	18.4 ± 0.4

Table 2. The ability characteristics of 316L SLM samples surface layers to resist mechanical contact action after and without heat treatment.

Treatment	δA (%)	R (%)	H_{IT}/E^*	H_{IT}^3/E^{*2} (GPa)
Without HT	86	12.1	0.019	0.001
After HT	89	9.8	0.014	0.001

The results of the microindentation that have been discussed above support the data on measuring the microhardness applying the recovered indentation technique which shows a slight softening of the SLM steel resulting from the heat treatment. It is shown by lowering the strength characteristics by 5-16%. In addition, it was found that the fraction of the elastic deformation in the total deformation decreases, indicating a faster transition of the heat-treated steel to plastic deformation under contact loading.

Therefore, the heat treatment that has been applied does not result in strengthening of the steel when the mechanism of aging austenite is employed. Deformation strengthening as well as chemothermal treatment leading to chemical modification of the surface layer might prove to be efficient for strengthening austenitic steel synthesized by SLM.

As the authors of the present paper have shown, efficient strengthening and improved tribological properties of metastable and deformation-stable austenitic chrome-nickel steels is achieved by processing with a sliding indenter [12-16] as well as by combining nanostructuring frictional

processing with low-temperature plasma nitriding [17-21]. It seems advantageous to use the described modifying processes for making a gradient-strengthened substrate on the surface of the synthesized austenitic steel for further application of nano-compositional thin-film multilayered coatings on the base of amorphous superhard diamond-like carbon and titanium carbides. We will study these directions in our future research, designed to give scientific credence for the new combined method for post-treatment of SLM samples. This method will make it possible to efficiently use thin-film high-strength coatings in additive manufacturing on parts made from structural steels that are significantly inferior in hardness to these coatings.

4. Conclusion

The austenitic structure with high densities of dislocations is formed by means of synthesizing a 316L steel by the selective laser melting technique. Heat treatment, quenching from 1050 °C and further 4-hour annealing at 480 °C, performed for degassing, reducing the number of vacancies and relaxing residual stresses do not result in altering the phase composition. However, a lower density of dislocations as well as their configurations in austenitic grains is evident. It causes a slight reduction of micromechanical characteristics to occur: the microhardness goes down by 5%, Martens hardness HM and indentation hardness at maximum load H_{IT} – by 12 and 16%, respectively. With the help of kinetic microindentation it was determined that the fraction of elastic deformation in the total deformation becomes smaller as caused by heat treatment. A 14% growth of the elasticity modulus E^* was discovered signifying a decrease of the porosity of the steel when heated to a high temperature.

Thus, the studied heat treatment does not provide strengthening through aging austenite in a synthesized steel. To obtain its effective strengthening application of nanostructuring frictional and chemicothermal (plasma nitriding) treatments may turn out to be advantageous as well as additional laying of thin-film coatings on a hardened substrate.

Acknowledgments

The main results were funded by the RFBR and Sverdlovsk Oblast, project number 20-48-660065. The results of the electron diffraction phase analysis were obtained by the M.N. Mikheev Institute of Metal Physics of the Ural Branch of the Russian Academy of Sciences (IMP UB RAS) within the state assignment of Ministry of Science and Higher Education of the Russian Federation (theme “Structure” No. № AAAA-A18-118020190116-6). The studies were performed at the collaborative access center “Testing center of nanotechnology and advanced materials” of IMP UB RAS.

References

- [1] Yap C Y, Chual C K, Dong Z L, Liu Z H, Dong Z L, Zhang D Q, Loh L E and Sing S L 2015 *Appl. Phys. Rev.* **2** 041101
- [2] Zhou X, Wanga D, Liu X, Zhang D D, Qu S, Ma J, London G, Shen Z and Liu W 2015 *Acta Mater.* **98** 1
- [3] Oliver W C and Pharr J M 1992 *J. Mater. Res.* **7** 1564
- [4] Amato K N, Gaytan S M, Murr L E, Martienez E, Shindo P V, Hernandez J, Collins S and Medina F 2012 *Acta Mater.* **60** 2229
- [5] Pinkerton A J and Li L 2003 *Appl. Surf. Sci.* **208-209** 411
- [6] Bazaleeva K O, Tsvetkova E V and Balakirev E V 2016 *Vestn. Mosk. Gos. Tekh. Univ. im. N.E. Bauman, Mashinostr. (Herald of the Bauman Moscow State Tech. Univ., Mech. Eng.)* **5** 117 [in Russian]
- [7] Saeidi K, Gao X, Lofajc F, Kvetková L and Shen Z J 2015 *J. Alloys Compd.* **633** 463
- [8] Cheng Y T and Cheng C M 1998 *Appl. Phys. Lett.* **73** 614
- [9] Petrzhik M I and Levashov E A 2007 *Crystallogr. Rep.* **52** 966
- [10] ISO 14577–1:2002
- [11] Mayrhofer P H, Mitterer C and Musil J 2003 *Surf. Coat. Technol.* **174-175** 725

- [12] Kuznetsov V P, Makarov A V, Osintseva A L, Yurovskikh A S, Savrai R A, Rogovaya S A and Kiryakov A E 2011 *Strengthening Technologies and Coatings* **11** 16 [in Russian]
- [13] Makarov A V, Skorynina P A, Osintseva A L, Yurovskikh A S and Savrai R A 2015 *Obrab. Met. (Met. Work. Mat. Sci.)* **4** 80 [in Russian]
- [14] Makarov A V, Skorynina P A, Osintseva A L, Yurovskikh A S 2017 *Phys. Metals Metallogr.* **118** 1225
- [15] Savrai R A, Makarov A V, Malygina I Yu, Rogovaya S A and Osintseva A L 2017 *Diagnostics, Resource and Mechanics of Materials and Structures* **5** 43 [in Russian]
- [16] Makarov A V, Skorynina P A, Volkova E G and Osintseva A L 2020 *Met. Sci. Heat Treat.* **61** 764
- [17] Makarov A V, Gavrilov N V, Samoylova G V, Mamaev A S, Osintseva A L and Savrai R A 2017 *Obrab. Met. (Met. Work. Mat. Sci.)* **2** 55 [in Russian]
- [18] Makarov A V, Samoylova G V, Gavrilov N V, Mamaev A S, Osintseva A L, Kurennykh T E and Savrai R A 2017 *AIP Conf. Proc.* **1915** 030011
- [19] Lezhnin N V, Makarov A V, Gavrilov N V, Osintseva A L and Savrai R A 2018 *AIP Conf. Proc.* **2053** 040050
- [20] Makarov A V, Savrai R A, Skorynina P A and Volkova E G 2020 *Met. Sci. Heat Treat.* **62** 61
- [21] Zhidkov I S, Kukharensko A I, Makarov A V, Savrai R A, Gavrilov N V, Cholakh S O, and Kurmaev E Z 2020 *Surf. Coat. Technol.* **386** 125492